Kobe University Repository : Kernel

PDF issue: 2025-12-05

Modeling dissolved inorganic carbon considering submerged aquatic vegetation

Nakayama, K. ; Komai, K. ; Tada, K. ; Lin, H. C. ; Yajima, H. ; Yano, S. ; Hipsey, M. R. ; Tsai, J. W.

(Citation)
Ecological Modelling,431:109188

(Issue Date)
2020-09-01

(Resource Type)
journal article

(Version)
Accepted Manuscript

(Rights)
© 2020 Elsevier B.V.
This manuscript version is made available under the CC-BY-NC-ND 4.0 license
http://creativecommons.org/licenses/by-nc-nd/4.0/

(URL)
https://hdl.handle.net/20.500.14094/90007400

KOBE UNIVERSITY

Modelling dissolved inorganic carbon considering submerged aquatic vegetation

K Nakayama[1] K Komai[2] K Tada[3] HC Lin[1] H Yajima[4] S Yano[5] MR Hipsey[6] JW Tsai[7]

1 Graduate School of Engineering, Kobe University, 1-1 Rokkodai-cho Nada-ku, Kobe city, 658-8501, Japan

2 School of Earth, Energy and Environmental Engineering, Kitami Institute of Technology 165 Koen-cho Kitami, 090-8507, Japan

3 Chuden Engineering Consultants, 2-3-30 Deshio, Minami-ku, Hiroshima 734-8510, Japan Japan

4 Estuary Research Center, Shimane University, 1060 Nishikawatsu-cho, Matsue city, 690-8504, Japan

5 Graduate School of Engineering, Kyushu University, 744 Moto-oka Nishi-ku, Fukuoka 819-0395, Japan

6 Aquatic Ecodynamics, UWA School of Agriculture and Environment, The University of Western Australia, Australia

7 Department of Biological Science and Technology, China Medical University, Taiwan

Corresponding author: K Nakayama

Tel: +81788036056

E-mail: nakayama@phoenix.kobe-u.ac.jp

Address: Graduate School of Engineering, Kobe University, 1-1 Rokkodai-cho Nada-ku, Kobe city, 658-8501, Japan

Highlights

- Aquatic vegetation can contribute to carbon capture in a lagoon system.
- A Seasonal NEP (SNEP) model is presented to estimate the change in DIC.
- The model can be applied to estimate lagoon productivity with limited information.
- Model results highlight the importance of estimating residence time.
- The SNEP model proves benefit of seagrass restoration on effective carbon capture.

ABSTRACT:

Net absorption of CO_2 by vegetated coastal ecosystems has been revealed as a key mechanism to capture and store carbon via the renewal of epigeal stem and rhizome biomass. Submerged aquatic ecosystems, such as seagrass meadows, have been termed “blue carbon” ecosystems because they absorb CO_2 for their underwater growth. Irradiance and water temperature are significant factors controlling net ecological production (NEP) by seagrass. As seagrass tends to grow in calm coastal areas subject to water-column stratification, such as lagoons, a new method for evaluating NEP accurately to access blue carbon capture in these enclosed waters is required. This study aimed to develop a model to investigate thermal effects, considering irradiance, on changes in dissolved inorganic carbon dynamics in a lagoon system, and assessment of the model to understand controls on carbon dynamics in Komuke Lagoon, Japan. NEP was successfully modelled by verifying its robustness against field observations. Furthermore, the proposed model can be applied to assess and enhance the effectiveness of blue carbon capture and storage as part revegetation measures to mitigate against global warming.

Keywords: photosynthesis; respiration; net ecosystem production; lagoon; macrophyte

1. Introduction

Urgent adaptation and mitigation measures are required to address natural disasters, such as floods, droughts, extreme heat, and landslides, which have been increasing due to global warming (IPCC, 2014). Such action depends on effective adaptation and mitigation measures. Vegetated shallow regions have recently been revealed to absorb and capture carbon dioxide by submerged aquatic vegetation - a potential sink of anthropogenic carbon, termed “blue carbon” (Duarte et al., 2013). Nellmann (2009) showed the effectiveness of the net absorption of CO_2 by blue carbon ecosystems, and it has been demonstrated that about 55 % of the carbon fixed by photosynthetic activity on the Earth is in the form of blue carbon. Seagrass beds or meadows capture and store autochthonous carbon from primary production and allochthonous carbon loaded from other areas during the renewal of their epigeal stem and rhizome biomass (Kennedy et al., 2010; Fourqurean et al., 2012). Therefore, there is the possibility that CO_2 is captured and stored in large amounts in shallow water areas dominated by submerged aquatic vegetation (Macreadie et al, 2019). For example, Beer et al. (1997) demonstrated that eelgrass plays a great role in carbon fixation and Palacios et al. (2007) also demonstrated that seagrass meadows can be absorb CO_2 from the atmosphere. However, Short (1999) indicated the difficulty in predicting the impact of global climate change effects on seagrass communities, as it remains unclear how photosynthesis and the productivity of aquatic plants will react to changes in the physical conditions of aquatic ecosystems under a changing environment. Tada et al. (2018) demonstrated the potential for application of a three-dimensional hydrodynamic model to evaluate the release and absorption of CO_2 by eelgrass (*Zostera marina*) in Komuke Lagoon of Hokkaido Island in Japan (Shintani and Nakayama, 2010; Nakayama et al., 2012; Nakayama et al., 2014; Nakayama et al., 2016; Nakayama et al., 2019). In this study, an attempt was made to model Dissolved Inorganic Carbon (DIC) by simulating the effect of respiration and photosynthesis by eelgrass, where the CO_2 concentrations were estimated from DIC, Total Alkalinity (TA), water temperature and salinity by assuming a chemical equilibrium state (per Zeebe et al., 2001). As a result, while DIC in this lagoon varied in the range 300 μmol-C kg^{-1} to 1300 μmol-C kg^{-1}, photosynthesis was found to exceed respiration, which resulted in an estimated sink for DIC of 325 μmol-C kg^{-1} (Tada et al., 2018). Additionally, Tada et al. (2018) showed that the influence of water temperature on photosynthesis and respiration should be included in numerical models of DIC dynamics due to its significance controlling eelgrass productivity.

Growth due to photosynthesis in eelgrass has been investigated in many previous studies based on photon flux density (often termed “photosynthetically active irradiance”, PAR) estimates (see

review by Lee et al., 2007). A Jassby type equation was found to fit to growth rates in laboratory and field experiments (Drew et al., 1979; Goodman et al., 1995; Holmer et al.,2001; Marsh et al., 1986; Olesen et al., 1993; Touchette, 1999; Zimmerman et al., 1995; Zimmerman et al., 1997). However, the best model resoloving DIC changes in relation to photon flux density remains unresolved. For investigating the effect of eelgrass photosynthesis on DIC dynamics, it is necessary to measure daily changes in photon flux density, since DIC decreases greatly due to photosynthesis during the daytime with a smaller increase in DIC due to respiration during the night. Therefore, the duration of photon flux density has been shown to be more important than the light compensation point and light saturation point in evaluating eelgrass production rates (Dennison et al., 1982; Dennison et al., 1985). Additionally, Tada et al. (2018) revealed that accurate topography must also be resolved for evaluating variability in DIC, based on predictions using a three-dimensional hydrodynamic model. Overall, spatial distributions in underwater photon flux density, nutrients, turbidity, and physical conditions have all been revealed to contribute strongly to the net growth of eelgrass (Dennison et al.,1986). Beyond depth as a primary determinant of growth, turbidity plays a great role in the photosynthesis of submerged aquatic vegetation, as it increases light attenuation and reduces the photon flux density, which results in suppression of the growth of eelgrass (Dennison, 1987; Moore et al., 1997). This turbidity effect on productivity could be due to the effect of algal blooms reducing the effective underwater photon flux density due to a high water column light extinction rate (Borum, 1985), or due to excessive sediments brough about from inflows or resuspension (Adams et al., 2016). Therefore, it is necessary to develop a DIC model which can resolve changes in photon flux density precisely from the viewpoint of the suppression of photon flux density due to high turbidity or algae blooms.

The effect of eelgrass photosynthesis on DIC has be shown to create site-specific patterns. For example, in previous studies, the minimum light requirement has been investigated, showing large variability from 5 % to about 40 % of the maximum irradiance (Dennison et al.,1993; Koch et al., 1996; Olesen et al., 1993). Additionally, the optimal growth temperature of eelgrass has been shown to range broadly from 13 °C to 24 °C in temperate zones (Boström et al., 2004; Ibarra-Obando et al., 1987; Lee et al., 2005; Lee et al., 2006; Moore et al., 1996; Sand-Jensen, 1975; Sfriso et al., 1998; Watanabe et al., 2005). In tropical or subtropical zones, the optimal growth temperature of eelgrass has been shown to range from 16 °C to 30 °C (Biebl et al., 1971; Cabello-Pasini et al., 2003; Dennison, 1987; Drew, 1979; Evans et al., 1986; Marsh et al., 1986; Penhale, 1977). Therefore, it is necessary to model the effects of eelgrass photosynthesis and respiration

on DIC dynamics in order to reflect regional characteristics under different climates.

Related to respiration and photosynthesis of eelgrass, it has been revealed that seagrass growth and production can be limited by nutrients even though photon flux density is plentiful (Coleman et al., 1994; Dennison et al., 1987; Iizumi and Hattori, 1982; Murray et al., 1992; Orth, 1977; Orth et al., 1983; Short et al., 1995; Thursby et al., 1982; Van Lent et al., 1995; Williams et al., 1993). There are many studies that have related the growth rate of eelgrass to nutrient supply from the roots (Boström et al., 2004; Dennison et al., 1987; Iizumi et al., 1982; Jørgensen, 1982; Mazzella et al., 1986; Moore et al., 1996; Pedersen et al., 1993; Short, 1987). The contribution of sediment nutrients to eelgrass growth rates has been found to be equal or be more than that from the water column (Short et al., 1984; Pedersen et al., 1992). Furthermore, Capone (1982) showed that nutrient concentrations vary greatly due to the presence of eelgrass, and nutrient pools have been shown to have rapid turnover rates. However, Burkholder et al. (1992, 1994) demonstrated that high nutrient enrichment inhibited eelgrass growth due to carbon limitation, phosphorus limitation, or other internal nutrient imbalances leading to physiological effects (Burkholder et al., 1992; Burkholder et al., 1994). Zimmerman et al. (1987) demonstrated the application of a numerical model to evaluate how nutrients affect the ecological functions of eelgrass, including respiration and photosynthesis. Therefore, in the context of nutrient supply, it can again be said that it is necessary to develop a detailed and precise submerged aquatic vegetation model for evaluating CO_2 flux.

Aside from light, photosynthesis parameters change seasonally due to differences in growth rate and water temperatures (Dennison, 1987; Orth et al., 1986; Phillips et al., 1983), with water temperature considered the primary factor controlling seasonal growth (Bulthuis, 1987; Setchell, 1929). Martin et al. (2006) showed that net CO_2 flux increases with the seasonal increase in water temperatures in the Bay of Brest, Western Brittany, France, with similar patterns in net O_2 flux. However, very limited studies have investigated how this temperature variability affects DIC fluxes. As submerged aquatic vegetation tends to grow best in calm, stratified coastal areas such as enclosed bays and lagoons, methods resolving the interaction between hydrodynamics, vegetation and carbon are required for application to these types of ecosystems. Therefore, this study aims to investigate thermal effects, considering irradiance, on changes in DIC fluxes under nutrient-rich (non-limiting) conditions. We develop a simplified and practical model to understand DIC dynamics, based on easily measurable experimental data, that can be applied to estimate seasonal productivity. The model is verified through application to Komuke Lagoon, Japan, where it is used to estimate carbon uptake by eelgrass.

2. Method

2.1. Laboratory experiments

Komuke Lagoon is connected to the Sea of Okhotsk through a tidal inlet and has a volume of approximately 3,333,000 m^3 and a maximum water depth of 3 m (Fig. 1). Although the tidal range of the Sea of Okhotsk is approximately 1 m, the tidal range of Komuke Lagoon is only 0.5 m because of the narrow 15 m width of the tidal inlet. For this reason, calm water conditions are usual in Komuke Lagoon and the eelgrass population is widely distributed. A laboratory experiment evaluating photosynthesis was conducted with lagoon water and eelgrass collected on the 25th of June 2018 at the sampling point (44° 15′ 7.3″ E, 143° 30′ 38.9″ N) shown in Fig. 1. The experiment was conducted outdoors in fine weather using a transparent acrylic water tank with a depth of 150 cm, a width of 20 cm, and a length of 20 cm (Fig. 2). Four shoots of eelgrasses taken from the lagoon were deployed in the water tank. The roots of the eelgrass were covered with vinyl sheets to avoid oxygen consumption by oxygen-demanding substances contained in the sediment. The salinity of the water used in the experiment was 22 psu. The dimensions (leaf width, length, and thickness) of eelgrass used in experiment were measured before experimentation (Table 1).

Two thermometers (Eijkelkamp Co. Ltd., SERA Diver) and two light quantum loggers (JFE Advantec Co. Ltd., DEFI2-L) were deployed in the water tank, recording every ten minutes. The experiment started at night, when photosynthesis was inactive, and continued for twenty-four hours. To provide vertically uniform conditions for eelgrass in the water tank, the water was well mixed using a peristatic pump with a flow rate of 7 mL min^{-1} through a silicon tube with a diameter of 2 mm; the water was gently taken from an inlet at a height of 100 cm from the tank bottom through the silicon tube and discharged from an outlet at a height of 0 cm from the tank bottom. The uniformity of water quality profiles in the water tank was confirmed by measuring temperatures periodically.

Approximately 200 mL water samples were taken from the water tank into a Scott Duran bottle by syringe and tube apparatus every hour. After sampling, 200 μL of a saturated aqueous solution of mercuric chloride was quickly added to the sample to prevent biological activity. DIC and TA of the water sample was then measured using a Total Alkalinity meter (Kimoto Electronic Co. Ltd., ATT-15) within 2 hours of sampling. Titrant for volumetric analysis (Kanto Kagaku, Co. Ltd., 0.1 mol L^{-1} hydrochloric acid) was used for DIC and TA measurement by high accuracy titration. Additionally, a water tank experiment under the same conditions but without eelgrass

was conducted as a control experiment. Concentrations of NO_3-N, NO_2-N, NH_4-N, and PO_4-P in water samples were measured for each experiment using an auto-analyzer (BLTEC Co. Ltd., QuAAtro 2HR).

The wet weight, dry weight, and carbon content of four eelgrass used in the laboratory experiment were measured separately for leaves and stems. Dry weight was measured after heating by an electric oven at 105℃ for 24 hours. Approximately 2 mg of dried sample was ground using a mortar and pestle and elemental carbon content analyzed using a CHNS analyzer (Parkin Elmer Co. Ltd., 2400II) in CHN mode to estimate eelgrass biomass.

2.2. Evaluation of coefficients of NEP model

Photon flux density and water temperature were measured every 10 minutes. The 10-minute data were converted to 1-hour interval data. Nitrogen and phosphorus could limit eelgrass respiration and photosynthesis when sediment water NH_4^+, $NO_3^- + NO_2^-$ and PO_4^{3-} concentrations are lower than 0.1, 0.5 and 0.03 μM, respectively (Lee et al., 2007). We confirmed that nitrogen and phosphorus concentrations were sufficient and didn't limit the eelgrass respiration and photosynthesis (Table 2). Therefore, in this study, we decided to apply Eq. (1) for modelling Net Ecosystem Production by eelgrass (NEP) taking into account photon flux density and water temperature. A Jassby type equation and Arrhenius equation were applied to simulate photosynthesis related to photon flux density and water temperature (Staehr et al., 2011; Beca-Carretero et al., 2018; Burkholz et al., 2019), where NEPR refers to Net Ecosystem Production due to Respiration by eelgrass and NEPP to Net Ecosystem Production due to Photosynthesis by eelgrass:

$$\frac{d}{dt}(\mathrm{DIC}) = \Delta\mathrm{DIC} = R_A \exp\left(-\frac{E_{aR}}{T_w R}\right) - P_\Psi \tanh\left(\frac{\alpha_\Psi I}{P_\Psi}\right) R_P \exp\left(-\frac{E_{aP}}{T_w R}\right) \quad (1)$$
$$= -\mathrm{NEP} = \mathrm{NEPR} - \mathrm{NEPP}$$

where, DIC μmol L^{-1} is the dissolved inorganic carbon, R_A μmol kg^{-1} h^{-1} is the parameter for respiration, E_{aR} m^2 kg s^{-2} is the activation energy for respiration, T_w K is the water temperature, R m^2 kg s^{-2} K^{-1} is the Boltzmann constant (1.380649 x 10^{-23}), P_Ψ μmol kg^{-1} h^{-1} and α_Ψ m^2 s kg^{-1} h^{-1} are the parameters for photosynthesis, I μmol m^{-2} s^{-1} is the photon flux density, R_P is the parameter for photosynthesis, E_{aP} m^2 kg s^{-2} is the activation energy for photosynthesis.

Firstly, the parameters for the respiration term in Eq. (1), R_A μ mol kg^{-1} h^{-1} and E_{aR}, were obtained using the fact that photosynthesis activity is negligible from sunset to sunrise when photon flux density is zero. We calculated ΔDIC under three water temperatures: 12 °C, 20 °C

and 24 °C in order to evaluate the effect of the change in water temperature on eelgrass respiration in dark conditions. Secondly, the parameters for photosynthesis was obtained by considering photon flux density and using the R_A and E_{aR} for NEPR. Thirdly, we proposed an eelgrass Seasonal Net Ecosystem Production (SNEP) model using the photon flux density duration recorded in the field. Finally, we applied the SNEP model to estimate changes in DIC due to eelgrass in Komuke Lagoon.

3. Results

3.1. Biological characteristics of eelgrass

The dry weight and biomass (carbon content) of eelgrass used in the laboratory experiment are shown in Table 1 and nutrient concentrations in the lagoon water are shown in Table 2. The biomass shown in Table 1 was based on the carbon content per unit leaf area calculated from the elemental carbon content and measured size of eelgrass. It should be noted that one data point was not available due to a measurement error. Mean leaf biomass was about 288 g C using the leaf area of both sides of the leaf m^2. Although the concentration of NO_3-N, NO_2-N, NH_4-N, and PO_4-P decreased during the experiment, photosynthetic rates were not limited by nutrients because concentrations remained sufficiently high (Lee et al., 2007).

3.2. Thermal effect on NEP

Partial pressures of carbon dioxide in water (fCO_2) started increasing at 8:00 pm on the 25th of June, and fCO_2 decreased from 5:00 am on the 26th. DIC changed in a pattern similar to fCO_2 (Fig. 3). In contrast to the eelgrass experiments, in the control tank, DIC was almost constant, which suggests that water column photosynthesis and respiration due to organisms other than eelgrass, such as phytoplankton, were negligible in terms of changes in DIC. Also, since TA changed only slightly, we found that the eelgrass predominantly affected DIC rather than TA. The maximum photon flux density occurred at 11:00 am on the 26th, when water temperature had increased from 12 to 27 °C. ΔDIC (=-NEP) μmol kg^{-1} h^{-1} was negative from 5:00 am on the 25th to 5:00 pm on the 26th, which demonstrated positive net ecosystem production (Fig. 3f).

When NEP was plotted against photon flux density, NEP values showed different tendencies below and above 250 μmol m^{-2} s^{-1} (Fig. 4). Red circles in Fig. 4 indicate 5 samples from 7:00 am to 11:00 am on the 26th, and green circles indicate 5 samples from 0:00 pm to 4:00 pm on the 26th. Red and green circle samples were sampled under mean water temperature of 16 °C and 25 °C, respectively. Therefore, it is noted that mean water temperature is a key factor controlling the

tendencies of NEP, which suggests the development of a NEPP parameterization needs to include the effect of water temperature in Eq. (1).

3.3. Estimation of coefficients of NEPR

Values for R_A and E_{aR} were obtained by assuming that ΔDIC represents NEPR from 7:00 pm of the 25th to 3:00 am of the 26th and from 6:00 pm to 7:00 pm of the 26th when photosynthetic activity is negligible (Fig. 5). It should be noted that only data with the condition ΔDIC>0 was applied because the respiration term, NEPR, should be higher than zero. Since ΔDIC from the 25th to 26th of June in 2018 was obtained when the water temperature was about 20 °C, we conducted separate laboratory experiments on the 10th of September 2018 with different water temperature conditions. Finally, 9 validated samples were obtained, in which a significant difference was confirmed to exist at the 5 % level using a Kruskal Wallis test. Although there are some fluctuations evident in Figure 5, parameters for respiration could be obtained based on strong relationships with water temperature: R_A=1.04 x 10^{17} μmol kg^{-1} h^{-1} and E_{aR} =1.52 x 10^{-19} m^2 kg s^{-2} with R^2 = 0.68.

3.4. Estimation of coefficients of NEPP

By applying R_A=1.04 x 10^{17} μ mol kg^{-1} h^{-1} and E_{aR} =1.52 x 10^{-19} m^2 kg s^{-2} into NEPR of Eq. (1), NEPP was obtained using Eq. (2):

$$\mathrm{NEPP} = -\Delta\mathrm{DIC} + \mathrm{NEPR} = -\Delta\mathrm{DIC} + R_A \exp\left(-\frac{E_{aR}}{T_w R}\right) \quad (2)$$

and the relationship between photon flux density and NEPP is shown in Fig. 6.

To investigate thermal dependence of eelgrass photosynthesis, a value that ignores thermal effects, NEPP$_{noT}$, was plotted against photon flux density using Eq. (3) (solid lines in Fig. 6):

$$\mathrm{NEPP}_{noT} = P_\Psi \tanh\left(\frac{\alpha_\Psi I}{P_\Psi}\right) \quad (3)$$

when the parameters are given as $P_{\psi\ noT}$=21.5 μmol kg^{-1} h^{-1} and $\alpha_{\psi\ noT}$=21.5/200 m^2 s kg^{-1} h^{-1}, comparison between NEPP and NEPP$_{noT}$ revealed a large difference in the tendencies between afternoon (green) and morning (red) conditions; red circles represented water samples from temperatures ranging from 12 to 20 °C, and green circles from 22 to 27 °C. The higher the water temperature, the larger the NEPP and vice versa, which is similar to the differences in the tendencies of NEPR. Therefore, an attempt was made to correct for the effect of temperature on the parameters for photosynthetic activity, R_P and E_{aP}, using NEPP / NEPP$_{noT}$, (Fig. 7):

$$\frac{\mathrm{NEPP}}{\mathrm{NEPP}_{noT}} = R_P \exp\left(-\frac{E_{aP}}{T_w R}\right) \tag{4}$$

where R_P=2.30 x 10^7 and E_{aP} =0.69 x 10^{-19} m^2 kg s^{-2} were obtained with good agreement (R^2=0.92). To test whether water temperature and NEPP / $NEPP_{noT}$ originate from the same distribution, we applied a Kruskal Wallis test at the 5 % level. Significant differences were confirmed between water temperature and NEPP / $NEPP_{noT}$, thus we obtained parameters for Eq. (1) as R_A=1.04 x 10^{17} μmol kg^{-1} h^{-1}, E_{aR} =1.52 x 10^{-19} m^2 kg s^{-2}, P_ψ=21.5 μmol kg^{-1} h^{-1}, α_ψ=21.5/200 m^2 s kg^{-1} h^{-1}, R_P=2.30 x 10^7 and E_{aP} =0.69 x 10^{-19} m^2 kg s^{-2}.

3.5. Proposal of the SNEP model

Eq. (1) can not only be applied to analyze local-scale NEP, for example though coupling with a three-dimensional hydrodynamic model, but it can also be applied to estimate the long-term (seasonal) change in DIC in enclosed waterbodies. To this end, we propose a method to estimate Seasonal Net Ecosystem Production (SNEP) by adapting Eq. (1). To estimate SNEP, it is necessary to include the hourly change in DIC (Dennison et al., 1982; Dennison et al., 1985), and SNEP is defined by integrating Eq. (1) for one day:

$$\begin{aligned}\mathrm{SNEP} = -R_A \frac{1}{t_{1day}} \int \exp\left(-\frac{E_{aR}}{T_w R}\right) dt \\ + P_\Psi \frac{1}{t_{1day}} R_P \int \tanh\left(\frac{\alpha_\Psi \beta_I I_S}{P_\Psi}\right) \exp\left(-\frac{E_{aP}}{T_w R}\right) dt\end{aligned} \tag{5}$$

where, t_{1day} is the integration period (= 24 h), β_I is the effectiveness coefficient (0: no photon flux density to 1: maximum photon flux density), and I_S is the photon flux density at water surface.

By assuming that water temperature changes sinusoidally:

$$T_w = T_m + T_h = T_m + T_{h0} \sin\left(\frac{2\pi}{24} t - \frac{\pi}{2}\right) \tag{6}$$

Eq. (5) can be simplified to:

$$\mathrm{SNEP} \approx -R_A \exp\left(-\frac{E_{aR}}{T_m R}\right) \gamma_R + P_\Psi \exp\left(-\frac{E_{aP}}{T_m R}\right) \gamma_P \tag{7}$$

where

$$\gamma_R = \frac{1}{t_{1day}} \int \exp\left(\frac{E_{aR} T_h}{{T_m}^2 R}\right) dt \tag{8}$$

$$\gamma_P = \frac{1}{t_{1day}} \int \tanh\left(\frac{\alpha_\Psi \beta_I I_S}{P_\Psi}\right) \exp\left(\frac{E_{aP} T_h}{{T_m}^2 R}\right) dt \quad (9)$$

where, T_m Celsius degree is the daily mean water temperature, $T_h = T_w - T_m$, T_{h0} is the amplitude of water temperature in a day, and t h is the time from 0 to 24 h. It should be noted that it is necessary to include the influence of topographical and tidal effects on a specific location because the photon flux density reaching the canopy may change significantly due to changes in bathymetry and tides. These effects can be included by changing the value of β_I, which is the parameter for attenuation of photon flux density and is a function of the extinction coefficient for light attenuation (Dennison et al.,1986).

To estimate and project dissolved oxygen (DO) over the bottom in an enclosed bay, Nakayama et al., (2010) demonstrated the suitability of a conceptual DO model by taking into account residence time between the inside of the bay and the outer ocean (Okada and Nakayama, 2007; Okada et al., 2011; Sato et al., 2012). This study thus makes an attempt to propose a SNEP model to estimate DIC using the SNEP approach and accounting for water exchange (Fig. 8):

$$V_0 \frac{d}{dt}(\mathrm{DIC}_S) = -V_0 \mathrm{SNEP} - \left(Q_E + Q_R\right)\mathrm{DIC}_S + Q_E \mathrm{DIC}_{out} + Q_R \mathrm{DIC}_R \quad (10)$$

where, DIC_S μmol kg^{-1} is the monthly mean DIC, V_0 m^3 is the volume of the lagoon, Q_E m^3 s^{-1} is the exchange flux between a lake and the ocean, Q_R m^3 s^{-1} is the river discharge, DIC_R μmol kg^{-1} is DIC of a river, and DIC_{out} μmol kg^{-1} is the typical DIC concentration of the ocean. We note that this model assumes the net atmospheric exchange of CO_2 over the period of the calculation is negligible, which is supported by estimates from in situ fCO_2 values.

By assuming a steady state in Eq. (10) (i.e. the left term is zero), the change in DIC_S can be obtained as:

$$\Delta\mathrm{DIC}_S = \mathrm{DIC}_{stable} - \mathrm{DIC}_S = t_S \mathrm{SNEP} \quad (11)$$

$$t_S = \frac{V_0}{Q_E + Q_R} \quad (12)$$

$$\mathrm{DIC}_{stable} = \frac{Q_E \mathrm{DIC}_{out} + Q_R \mathrm{DIC}_R}{Q_E + Q_R} \quad (13)$$

where, $\Delta\mathrm{DIC}_S$ μmol kg^{-1} is the change in DIC with NEP, DIC_{stable} μmol kg^{-1} is DIC in a steady state without NEP (NEP = 0), and t_S h is the residence time of the target domain. In other words, if we obtain residence time, t_S, and SNEP, the change in DIC due to eelgrass can be estimated using Eq. (11), and used as a measure of system scale carbon uptake.

4. Discussion

In this study, we obtained parameters needed to simulate the response of photosynthesis to photon flux density and water temperature based on a Jassby type P-I equation and an Arrhenius equation (Staehr et al., 2011; Beca-Carretero et al., 2018; Burkholz et al., 2019). Lee et al. (2007) found that laboratory experiments tend to underestimate saturation irradiance because of the usage of leaf segments. Since we did not remove the roots in our laboratory experiments, the saturation irradiance was estimated as 200 μmol m^{-2} s^{-1} by $P_{\psi\ noT}$ / $\alpha_{\psi\ noT}$, where $P_{\psi\ noT}$=21.5 μmol kg^{-1} h^{-1} and $\alpha_{\psi\ noT}$=21.5/200 m^2 s kg^{-1} h^{-1}. The value is larger than the average level of saturation irradiance for leaf segments of *Zostera marina*, 116 μmol m^{-2} s^{-1}, while the average value of saturation irradiance for whole plant is 450 μmol m^{-2} s^{-1} (Lee et al., 2007).

The rate of change in NEP due to photosynthesis and respiration has been shown to increase with increasing water temperature (Dennison, 1987; Orth et al., 1986; Phillips et al., 1983; Bulthuis, 1987; Setchell, 1929). To understand thermal dependencies, NEPP, NEPR and NEP were computed by changing water temperatures from 5 °C to 30 °C using Eq. (1) (Fig. 9). NEPP and NEPR increased with the increasing water temperature (Fig. 9a and Fig. 9b). When the photon flux density was more than about 250 μ mol m^{-2} s^{-1}, NEPP varied from 8 μ mol kg^{-1} h^{-1} to 34 μ mol kg^{-1} h^{-1}, an increase of 26 μ mol kg^{-1} h^{-1} (Fig. 9a). In comparison, NEP under a thermal increase from 5 to 30 °C varied from 7 μ mol kg^{-1} h^{-1} to 17 μ mol kg^{-1} h^{-1}, an increase of 10 μ mol kg^{-1} h^{-1} (Fig. 9c). Furthermore, when photon flux density was more than 250 μ mol m^{-2} s^{-1}, NEP was almost constant under a thermal increase from 25 to 30 °C because the increase in NEPR was almost equal to the increase in NEPP (Fig. 9c). Lee et al. (2007) revealed that the average value of optimal temperature of *Zostera marina* is about 15 °C for growth and 23 °C for photosynthesis, which is in good agreement with our study with optimal temperatures of about 25 °C for photosynthesis.

We applied the SNEP model to Komuke Lagoon to explore the applicability for the evaluation of seasonal changes in DIC. We referred to the field observations which were conducted in Komuke Lagoon in May 2013 (Tada et al., 2018) and August 2018. May and August were chosen as target months in order to clarify the seasonal effect of the difference in water temperature between spring and summer. Firstly, γ_R and γ_P for SNEP were estimated from Eqs. (8) and (9) by giving 5 different β_I: 100 %, 75%, 50 %, 25 % and 10 % (Table 3). This showed that γ_P varied greatly with the change in β_I. In contrast to β_I, the difference in photon flux density between May and August was negligible and the values for γ_P were the same between the two seasons. Since eelgrass meadows exist from the bottom to a water depth of about 1.0 m in Komuke

Lagoon, and the extinction coefficient was about 2.0 m^{-1} including the effect of turbidity with a mean water depth of 2.0 m, β_I was obtained as 25 % using Eq. (14):

$$\beta_I = \frac{1}{h_m}\int_0^{l_E} \exp[-k_E(h_m - z)]dz \quad (14)$$

where, h_m m is the mean water depth, k_E m^{-1} is the extinction coefficient, and l_E m is the deflected vegetation height.

SNEP was computed against water temperature, T_w, from β_I = 0 % to β_I = 100 % (Fig. 10). Although the SNEP did not change much from β_I = 50 % to β_I = 100 %, SNEP decreases greatly from β_I = 50 % to β_I = 0 %. When β_I was 25 %, a peak in SNEP appeared at a water temperature of 15 °C and SNEP became negative when the water temperature was more than 28 °C. Watanabe et al. (2005) demonstrated that optimal temperature for *Zostera marina* is 16.1 °C in Akkeshi Bay, which is located close to Komuke Lagoon. This may suggest the practical applicability of the relatively simple SNEP model for real field environments. Tada et al. (2018) revealed that DIC at the water surface, DIC_S, was smaller than the no eelgrass stable condition, DIC_{stabl}, in Komuke Lagoon on the 15th of May 2013 using a three-dimensional hydrodynamic model, which shows $\Delta DIC_S = DIC_{stabl} - DIC_S$ = 325 μ mol kg^{-1} (Table 4). The residence time of Komuke Lagoon was t_S = 110 h and the mean water temperature was 7.1 °C. Since SNEP is 2.82 μ mol kg^{-1} h^{-1} from Fig. 10, t_S SNEP can be obtained as 310 μ mol kg^{-1}. Therefore, the estimated t_S SNEP = 310 μ mol kg^{-1} approximately agreed with ΔDIC_S = 325 μ mol kg^{-1}, which suggests the applicability of the SNEP model to an enclosed waterbody, when the residence time is known.

In addition to the estimation of t_S SNEP in May 2013, we conducted water sampling at the water surface in Komuke Lagoon and measured water temperature, salinity and DIC in 2018 in order to investigate the applicability of the SNEP model Eq. (11) (sampling stations are shown in Fig. 1). It should be noted that we found no significant differences in water quality and flow fields between 2013 and 2018 since Komuke Lagoon has a very narrow inlet and the Okhotsk Sea provides stable periodic annual changes in water quality. The mean water temperature was 23.5 °C, which corresponds to SNEP = 2.23 μ mol kg^{-1} h^{-1} using β_I = 25 % from Fig. 10 (Table 4). As the residence time is about 110 h, t_S SNEP was found to be 245 μ mol kg^{-1}. Using the low-salinity endmember of rivers and the high-salinity endmember of the ocean, ΔDIC_S was estimated as 255 μ mol kg^{-1} from field observations following Zeebe et al. (2001). Again, the estimated t_S SNEP = 245 μ mol kg^{-1} agreed well with ΔDIC_S = 255 μ mol kg^{-1} from the field observations. The proposed SNEP model is specific to enclosed or semi-enclosed waterbodies and not for suitable for the open ocean because of the requirement to evaluate residence times. Since eelgrass appears to be

adapted to calm conditions, and there is the possibility to obtain residence times accurately for these waterbodies, this suggests the SNEP model can be useful to improve predictions of carbon capture and storage by eelgrass populations in protected waters.

5. Conclusion

Aiming to understand the NEP of eelgrass in Komuke Lagoon, which is located in the east of Hokkaido, parameters for NEPR were obtained as R_A=1.04 x 10^{17} μ mol kg^{-1} h^{-1} and E_{aR} =1.52 x 10^{-19} m^2 kg s^{-2} using the hourly change in DIC without photon flux density in laboratory experiments. The photosynthetic activity of eelgrass was confirmed to be affected by water temperature from laboratory experiments, and parameters for NEPP were obtained as P_ψ=21.5 μ mol kg^{-1} h^{-1}, α_ψ=21.5/200 m^2 s kg^{-1} h^{-1}, R_P=2.30 x 10^7 and E_{aP} =0.69 x 10^{-19} m^2 kg s^{-2}. The SNEP model was proposed, in which the seasonal change in DIC, ΔDIC_S, can be estimated as t_S SNEP by using the residence time, t_S. The SNEP model was applied to two sets of field observations from Komuke Lagoon, May 2013 and August 2018, and the estimated seasonal change in DIC, t_S SNEP, was confirmed to agree with ΔDIC_S from field observations. In other words, the seasonal change in NEP can be obtained as ΔDIC_S / t_S using the residence time, t_S, and the seasonal change in DIC, ΔDIC_S, from endmember analysis using field observations. Since the development and implementation of mitigation measures against global warming is an urgent issue, the proposed SNEP model in this study may be applied to assist efforts to enhance effective capture and storage of carbon dioxide through seagrass restoration. Also, the SNEP model may be useful for assessing changes due to climate change, e.g. as a screening tool to investigate whether the warming trend improves net productivity or not with limited information.

412 Acknowledgments
413 This work was supported by the Japan Society for the Promotion of Science under grant
414 18H01545 and 18KK0119.
415
416

References

1) IPCC, 2014. Climate Change 2014: Synthesis Report. Contribution of Working Groups I, II and III to the Fifth Assessment Report of the Intergovernmental Panel on Climate Change [Core Writing Team, R.K. Pachauri and L.A. Meyer (eds.)]. IPCC, Geneva, Switzerland, 151 pp.

2) Adams, M. P., Hovey, R. K., Hipsey, M. R., Bruce, L. C., Ghisalberti, M., Lowe, R. J., Gruber, R. K., Ruiz-Montoya, L., Maxwell, P. S., Callaghan, D. P., Kendric, G. A., O'Brien, K. R., 2016. Feedback between sediment and light for seagrass: Where is it important? Limnol. Oceanogr. 61, 1937-1955.

3) Beca-Carretero, P., Olesen, B., Marba, N., Krause-Jensen, D., 2018. Response to experimental warming in northern eelgrass populations: comparison across a range of temperature adaptations. Mar. Ecol. Prog. Ser. 589, 59–72.

4) Beer, S., Rehnberg, J., 1997. The acquisition of inorganic carbon by the seagrass *Zostera marina*. Aquat. Bot. 56, 277–283.

5) Biebl, R., McRoy, C.P., 1971. Plasmatic resistance and rate of respiration and photosynthesis of *Zostera marina* at different salinities and temperatures. Mar. Biol. 8, 48–56.

6) Borum, J., 1985. Development of epiphytic communities on eelgrass (*Zostera marina*) along a nutrient gradient in a Danish estuary. Mar. Biol. 87, 211–218.

7) Boström, C., Roos, C., Rönnberg, O., 2004. Shoot morphometry and production dynamics of eelgrass in the northern Baltic Sea. Aquat. Bot. 79, 145–161.

8) Bulthuis, D.A., 1987. Effects of temperature on photosynthesis and growth of seagrasses. Aquat. Bot. 27, 27–40.

9) Burkholder, J.M., Glasgow Jr., H.B., Cooke, J.E., 1994. Comparative effects of water-column nitrate enrichment on eelgrass *Zostera marina*, shoalgrass *Halodule wrightii*, and widgeongrass *Ruppia maritima*. Mar. Ecol. Prog. Ser. 105, 121–138.

10) Burkholder, J.M., Mason, K.M., Glasgow Jr., H.B., 1992. Water-column nitrate enrichment promotes decline of eelgrass *Zostera marina*: evidence from seasonal mesocosm experiments. Mar. Ecol. Prog. Ser. 81, 163–178.

11) Burkholz, C., Duarte, C.M., Garcias-Bonet, N., 2019. Thermal dependence of seagrass ecosystem metabolism in the Red Sea. Mar. Ecol. Prog. Ser. 614, 79–90.

12) Cabello-Pasini, A., Muñiz-Salazar, R., Ward, D.H., 2003. Annual variations of biomass and photosynthesis in *Zostera marina* at its southern end of distribution in the North Pacific. Aquat. Bot. 76, 31–47.

13) Capone, D.G., 1982. Nitrogen fixation (acetylene reduction) by rhizosphere sediments of the eelgrass *Zostera marina*. Mar. Ecol. Prog. Ser. 10, 67–75.
14) Coleman, V.L., Burkholder, J.M., 1994. Community structure and productivity of epiphytic microalgae on eelgrass (*Zostera marina* L.) under water-column nitrate enrichment. J. Exp. Mar. Biol. Ecol. 179, 29–48.
15) Dennison, W.C., 1987. Effects of light on seagrass photosynthesis, growth and depth distribution. Aquat. Bot. 27, 15–26.
16) Dennison, W.C., Alberte, R.S., 1982. Photosynthetic responses of *Zostera marina* L. (eelgrass) to in situ manipulations of light intensity. Oecologia 55, 137–144.
17) Dennison, W.C., Alberte, R.S., 1985. Role of daily light period in the depth distribution of *Zostera marina* (eelgrass). Mar. Ecol. Prog. Ser. 25, 51–61.
18) Dennison, W.C., Alberte, R.S., 1986. Photoadaptation and growth of *Zostera marina* L. (eelgrass) transplants along a depth gradient. J. Exp. Mar. Biol. Ecol. 98, 265–282.
19) Dennison, W.C., Aller, R.C., Alberte, R.S., 1987. Sediment ammonium availability and eelgrass (*Zostera marina*) growth. Mar. Biol. 94, 469–477.
20) Dennison, W.C., Orth, R.J., Moore, K.A., Stevenson, J.C., Carter, V., Kollar, S., Bergstrom, P.W., Batiuk, R.A., 1993. Assessing water quality with submersed aquatic vegetation. Bioscience 43, 86–94.
21) Drew, E.A., 1979. Physiological aspects of primary production in seagrasses. Aquat. Bot. 7, 139–150.
22) Duarte, C.M., Losada, I.J., Hendriks, I.E., Mazarrasa, I., and Marbà, N., 2013. The role of coastal plant communities for climate change mitigation and adaptation. Nature Climate Change, 3(11), 961.
23) Evans, A.S., Webb, K.L., Penhale, P.A., 1986. Photosynthetic temperature acclimation in two coexisting seagrasses, *Zostera marina* L. and *Ruppia maritima* L. Aquat. Bot. 24, 185–197.
24) Fourqurean J.W, Duarte, C.M., Kennedy H., Marbà, N., Holmer, M., Mateo, M.A., Apostolaki, E.T., Kendrick, G.A., Krause-Jensen, D., McGlathery, K.J., Serrano, O., 2012. Seagrass ecosystems as a globally significant carbon stock. Nat. Geosci. 5, 505–509.
25) Goodman, J.L., Moore, K.A., Dennison, W.C., 1995. Photosynthetic responses of eelgrass (*Zostera marina* L.) to light and sediment sulfide in a shallow barrier island lagoon. Aquat. Bot. 50, 37–47.
26) Holmer, M., Bondgaard, E.J., 2001. Photosynthetic and growth response of eelgrass to low oxygen and high sulfide concentrations during hypoxic events. Aquat. Bot. 70, 29–38.

27) Ibarra-Obando, S.E., Huerta-Tamayo, R., 1987. Blade production of *Zostera marina* L. during the summer-autumn period on the pacific coast of Mexico. Aquat. Bot. 28, 301–315.
28) Iizumi, H., Hattori, A., 1982. Growth and organic production of eelgrass (*Zostera marina* L.) in temperate waters of the Pacific coast of Japan. III. The kinetics of nitrogen uptake. Aquat. Bot. 12, 245–256.
29) Iizumi, H., Hattori, A., McRoy, C.P., 1982. Ammonium regeneration and assimilation in eelgrass (*Zostera marina*) beds. Mar. Biol. 66, 59–65.
30) Jørgensen, B.B., 1982. Mineralization of organic matter in the sea bed—the role of sulphate reduction. Nature 296, 643–645.
31) Kennedy, H., Beggins, J., Duarte, C.M., et al., 2010. Seagrass sediments as a global carbon sink: isotopic constraints. Glob. Biogeochem. Cy. 24:GB4026.
32) Koch, E.W., Beer, S., 1996. Tides, light and the distribution of *Zostera marina* in Long Island Sound, USA. Aquat. Bot. 53, 97–107.
33) Lee, K.-S., Park, S.R., Kim, J.-B., 2005. Production dynamics of the eelgrass, *Zostera marina* in two bay systems on the south coast of the Korean peninsula. Mar. Biol. 15.0, 1091–1108.
34) Lee, K.S., Park, S.R., Kim, Y.K., 2007. Effects of irradiance, temperature, and nutrients on growth dynamics of seagrasses: A review. J. Exp. Mar. Biol. Ecol. 350, 144–175.
35) Lee, S.Y., Kim, J.B., Lee, S.M., 2006. Temporal dynamics of subtidal *Zostera marina* and intertidal *Zostera japonica* on the southern coast of Korea. Mar. Ecol. 27, 133–144.
36) Macreadie, P.I., Anton, A., Raven, J.A., Beaumont, N., Connolly, M., Friess, D.A., … Duarte, C.M., 2019. The future of Blue Carbon science, Nature Communicationsvolume 10, Article number: 3998.
37) Marsh Jr., J.A., Dennison, W.C., Alberte, R.S., 1986. Effects of temperature on photosynthesis and respiration in eelgrass (*Zostera marina L.*). J. Exp. Mar. Biol. Ecol. 101, 257–267.
38) Martin, S., Castets, M.D., Clavier, J., 2006. Primary production, respiration and calcification of the temperate free-living coralline alga *Lithothamnion corallioides*. Aquat. Bot. 85, 121–128.
39) Mazzella, L., Alberte, R.S., 1986. Light adaptation and the role of autotrophic epiphytes in primary production of the temperate seagrass, *Zostera marina* L. J. Exp. Mar. Biol. Ecol. 100, 165–180.
40) Moore, K.A., Neckles, H.A., Orth, R.J., 1996. *Zostera marina* (eelgrass) growth and survival along a gradient of nutrients and turbidity in the lower Chesapeake Bay. Mar. Ecol. Prog. Ser.

142, 247–259.
41) Moore, K.A., Wetzel, R.L., Orth, R.J., 1997. Seasonal pulses of turbidity and their relations to eelgrass (*Zostera marina* L.) survival in an estuary. J. Exp. Mar. Biol. Ecol. 215, 115–134.
42) Murray, L., Dennison, W.C., Kemp, W.M., 1992. Nitrogen versus phosphorus limitation for growth of an estuarine population of eelgrass (*Zostera marina* L.). Aquat. Bot. 44, 83–100.
43) Nakayama, K., Nguyen, H.D., Shintani, T., Komai, K., 2016. Reversal of secondary circulations in a sharp channel bend. Coas. Eng. J. 58, 1650002.
44) Nakayama, K., Sato, T., Shimizu, K., Boegman, L., 2019. Classification of internal solitary wave breaking over a slope. Phys. Rev. Fluids. 4, 014801.
45) Nakayama, K., Shintani, T., Kokubo, K., Kakinuma, T., Maruya, Y., Komai, K., Okada, T., 2012. Residual current over a uniform slope due to breaking of internal waves in a two-layer system. J. Geophys. Res. 117, C10002, 1-11.
46) Nakayama, K., Shintani, T., Shimizu, K., Okada, T., Hinata, H., Komai, K., 2014. Horizontal and residual circulations driven by wind stress curl in Tokyo Bay. J. Geophys. Res. 119, 1977-1992.
47) Nakayama, K., Sivapalan, M., Sato, C., Furukawa, K., 2010. Stochastic characterization of the onset of and recovery from hypoxia in Tokyo Bay, Japan: Derived distribution analysis based on “strong wind” events, Wat. Resour. Res. 46, W12532, 1-15.
48) Nellemann C., Corcoran E., Duarte C.M., Valdes L., DeYoung C., Fonseca L., Grimsditch G., 2009. Blue Carbon. A Rapid Response Assessment. United Nations Environmental Programme, GRID-Arendal, Birkeland.
49) Okada, T., Nakayama, K., 2007. Modeling of dissolved oxygen in an enclosed bay with sill, J. Environ. Eng. - ASCE, 1(1), 104.
50) Okada, T., Nakayama, K., Takao, T., Furukawa, K., 2011. Influence of freshwater input and bay reclamation on long-term changes in seawater residence times in Tokyo Bay, Japan, Hydrological Processes, 24, 2694-2702.
51) Olesen, B., Sand-Jensen, K., 1993. Seasonal acclimatization of eelgrass *Zostera marina* growth to light. Mar. Ecol. Prog. Ser. 94, 91–99.
52) Orth, R.J., 1977. Effect of nutrient environment on growth of the eelgrass *Zostera marina* in the Chesapeake Bay, Virginia, USA. Mar. Biol. 44, 187–194.
53) Orth, R.J., Moore, K.A., 1983. Chesapeake Bay: an unprecedented decline in submerged aquatic vegetation. Science 222, 51–53.
54) Orth, R.J., Moore, K.A., 1986. Seasonal and year-to-year variations in the growth of *Zostera*

549 *marina* L. (eelgrass) in the lower Chesapeake Bay. Aquat. Bot. 24, 335–341.
550 55) Palacios, S.L., Zimmerman, R.C., 2007. Response of eelgrass *Zostera marina* to CO2
551 enrichment: possible impacts of climate change and potential for remediation of coastal
552 habitats. Mar. Ecol. Prog. Ser. 344, 1–13.
553 56) Pedersen, M.F., Borum, J., 1992. Nitrogen dynamics of eelgrass *Zostera marina* during a late
554 summer period of high growth and low nutrient availability. Mar. Ecol. Prog. Ser. 80, 65–73.
555 57) Pedersen, M.F., Borum, J., 1993. An annual nitrogen budget for a seagrass *Zostera marina*
556 population. Mar. Ecol. Prog. Ser. 101, 169–177.
557 58) Penhale, P.A., 1977. Macrophyte-epiphyte biomass and productivity in an eelgrass (*Zostera*
558 *marina* L.) community. J. Exp. Mar. Biol. Ecol. 26, 211–224.
559 59) Phillips, R.C., McMillan, C., Bridges, K.W., 1983. Phenology of eelgrass, *Zostera marina*
560 L., along latitudinal gradients in North America. Aquat. Bot. 15, 145–156.
561 60) Sand-Jensen, K., 1975. Biomass, net production and growth dynamics in an eelgrass (*Zostera*
562 *marina* L.) population in Vellerup Vig, Denmark. Ophelia 14, 185–201.
563 61) Satoh, C., Nakayama, K., Furukawa, K., 2012. Contributions of wind and river effects on
564 DO concentration in Tokyo Bay, Estuarine Coast and Shelf Science, 109, 91-97.
565 62) Setchell,W.A., 1929.Morphological and phenological notes on *Zostera marina* L. Univ. Calif.
566 Publ. Bot. 14, 389–452.
567 63) Sfriso, A., Ghetti, P.F., 1998. Seasonal variation in biomass, morphometric parameters and
568 production of seagrasses in the lagoon of Venice. Aquat. Bot. 61, 207–223.
569 64) Shintani, T., Nakayama, K., 2010. An object-oriented approach to environmental fluid
570 modeling. The 21st International Symposium on Transport Phenomena.
571 65) Short, F.T., 1987. Effects of sediment nutrients on seagrasses: literature review and
572 mesocosm experiment. Aquat. Bot. 27, 41–57.
573 66) Short, F.T., Burdick, D.M., Kaldy, J.E., 1995. Mesocosm experiments quantify the effects of
574 eutrophication on eelgrass, *Zostera marina*. Limnol. Oceanogr. 40, 740–749.
575 67) Short, F.T., McRoy, C.P., 1984. Nitrogen uptake by leaves and roots of the seagrass *Zostera*
576 *marina* L. Bot. Mar. 27, 547–555.
577 68) Short, F.T., Neckles, H.A., 1999. The effects of global climate change on seagrasses. Aquat.
578 Bot. 63, 169–196.
579 69) Staehr, P.A., Borum, J., 2011. Seasonal acclimation in metabolism reduces light requirements
580 of eelgrass (*Zostera marina*). J. Exp. Mar. Biol. Ecol. 407, 139–146.
581 70) Tada, K., Nakayama, K., Komai, K., Tsai, J.W., Sato, Y., Kuwae, T., 2018. Analysis of

582 dissolved inorganic carbon due to seagrass in a stratified flow. J. Japan Soc. Civil Eng., Ser.
583 B3. 74, 444-449.
584 71) Thursby, G.B., Harlin, M.M., 1982. Leaf–root interaction in the uptake of ammonia by
585 *Zostera marina*. Mar. Biol. 72, 109–112.
586 72) Touchette, B.W., 1999. Physiological and developmental responses of eelgrass (*Zostera*
587 *marina* L.) to increases in water-column nitrate and temperature. Ph.D. Dissertation, North
588 Carolina State University, Raleigh, NC.
589 73) Van Lent, F., Verchuure, J.M., van Veghel, L.J., 1995. Comparative study on populations of
590 *Zostera marina* L. (eelgrass): in situ nitrogen enrichment and light manipulation. J. Exp. Mar.
591 Biol. Ecol. 185, 55–76.
592 74) Watanabe, M., Nakaoka, M., Mukai, H., 2005. Seasonal variation in vegetative growth and
593 production of the endemic Japanese seagrass Zostera asiatica: a comparison with sympatric
594 *Zostera marina*. Bot. Mar. 48, 266–273.
595 75) Williams, S.L., Ruckelshaus,M.H., 1993. Effects of nitrogen availability and herbivory on
596 eelgrass (*Zostera marina*) and epiphytes. Ecology 74, 904–918.
597 76) Zeebe, R.E., Wolf-Gladrow, D., 2001. Equilibrium. In: CO2 in Seawater: Equilibrium,
598 Kinetics, Isotopes. Elsevier, Amsterdam, 1–83.
599 77) Zimmerman, R.C., Kohrs, D.G., Steller, D.L., Alberte, R.S., 1997. Impacts of CO2
600 enrichment on productivity and light requirements of eelgrass. Plant Physiol. 115, 599–607.
601 78) Zimmerman, R.C., Reguzzoni, J.L., Alberte, R.S., 1995. Eelgrass (*Zostera marina* L.)
602 transplants in San Francisco Bay: role of light availability on metabolism, growth and
603 survival. Aquat. Bot. 51, 67–86.
604 79) Zimmerman, R.C., Smith, R.D., Alberte, R.S., 1987. Is growth of eelgrass nitrogen limited?
605 A numerical simulation of the effects of light and nitrogen on the growth dynamics of *Zostera*
606 *marina*. Mar. Ecol. Prog. Ser. 41, 167–176.
607

608 Figure

609

610 Fig. 1 Sampling stations in Komuke Lagoon

611

612 Fig. 2. Schematic diagram of the laboratory experiment tank containing eelgrass

613

614 Fig. 3. Laboratory experiment results from 21:00 on the 25th to 19:00 on the 26th of June 2018.
615 (a) fCO_2 with and without eelgrass. (b) DIC with and without eelgrass. (c) TA with and without
616 eelgrass. (d) photon flux density. (e) water temperature. (f) ΔDIC.

617

618 Fig. 4. Photon flux density and NEP.

619

620 Fig. 5. Water temperature and ΔDIC. Solid line is the first term of equation (1).

621

622 Fig. 6. Photon flux density and NEPP by equation (2). Solid line is equation (3).

623

624 Fig. 7. Water temperature and the ratio of NEPP and $NEPP_{noT}$. Solid line is equation (4).

625

626 Fig. 8. Schematic diagram of SNEP model.

627

628 Fig. 9. Effect of water temperature on (a) NEPP, (b) NEPR and (c) NEP.

629

630 Fig. 10. Water temperature and DNEP in Komuke Lagoon.

631

632

633

Table

Table 1. Specimens in laboratory experiments.

Table 2. Nutrient concentrations in experimental water.

Table 3. γ_R and γ_P in May 2013 and August 2018.

Table 4. Field observations in Lake Komuke.

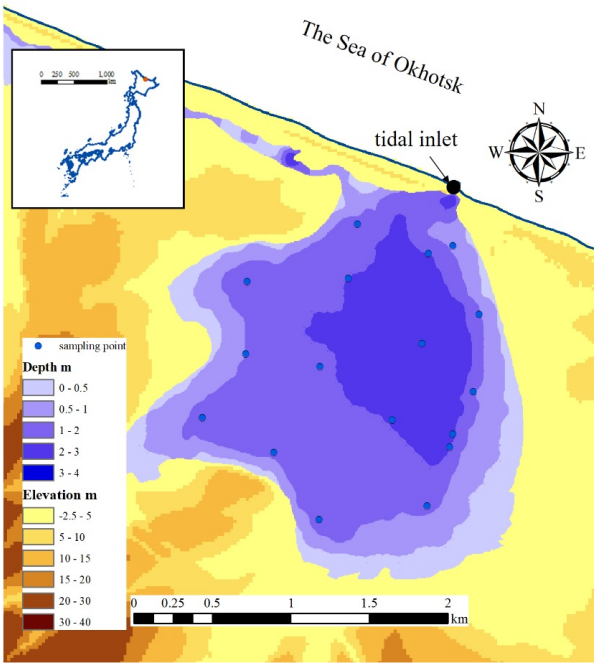

Fig. 1 Sampling stations in Komuke Lagoon

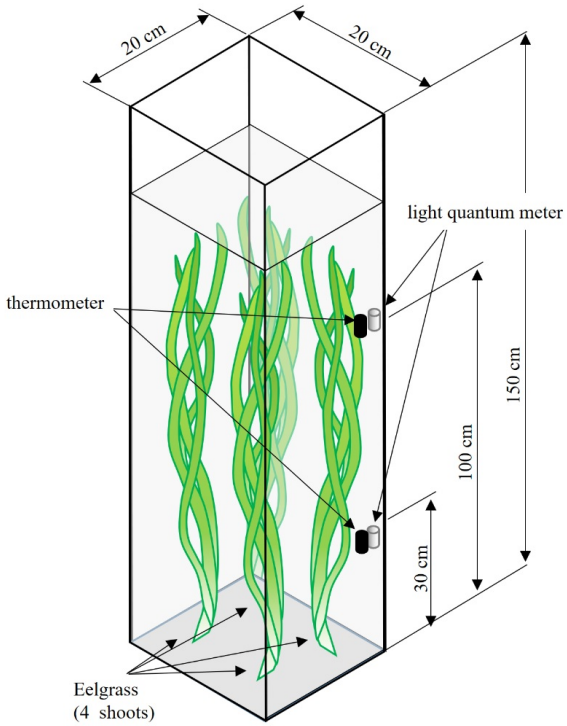

Fig. 2. Schematic diagram of the laboratory experiment tank containing eelgrass

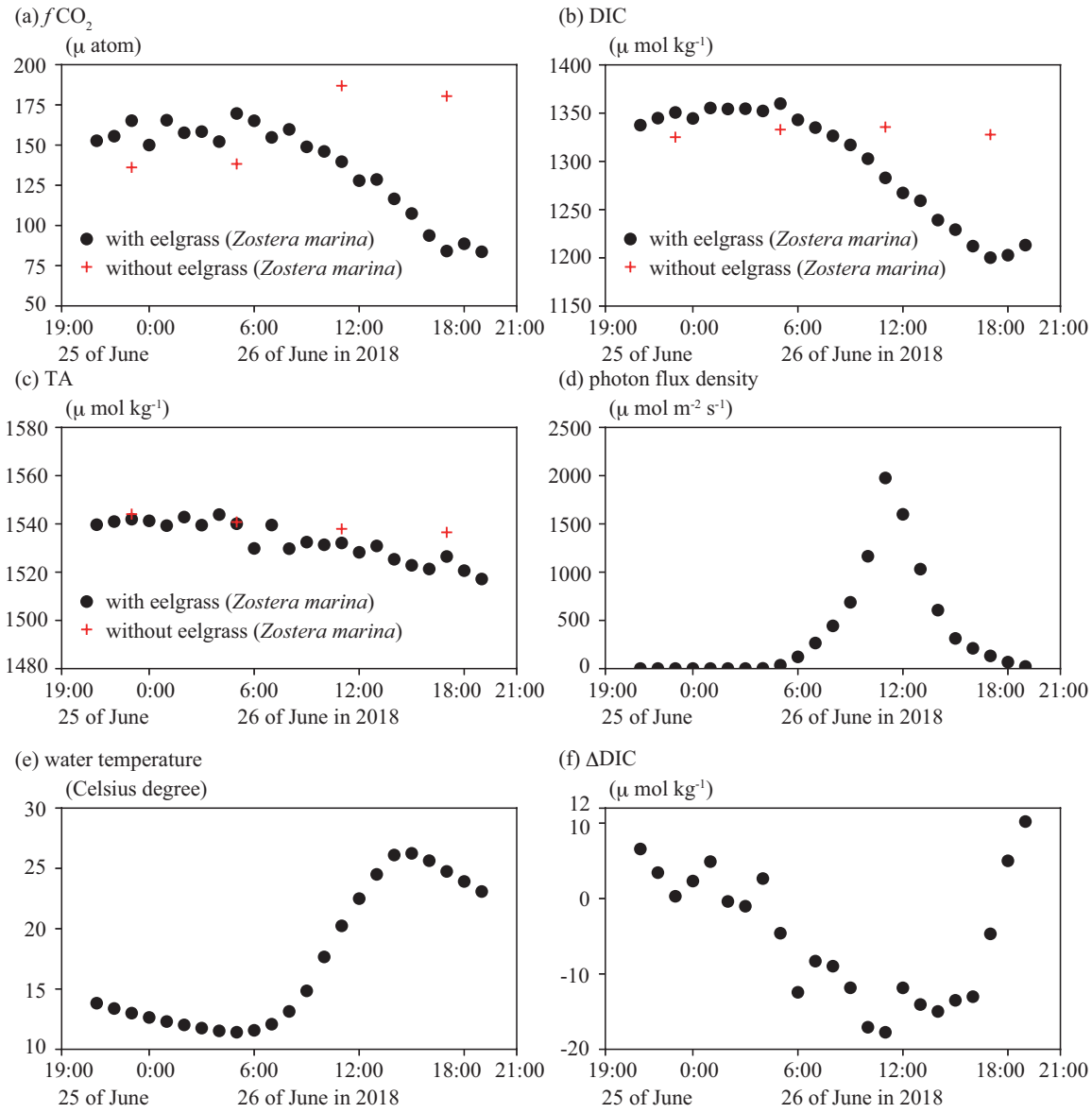

Fig. 3. Laboratory experiment results from 21:00 on the 25th to 19:00 on the 26th of June 2018. (a) fCO_2 with and without eelgrass. (b) DIC with and without eelgrass. (c) TA with and without eelgrass. (d) photon flux density. (e) water temperature. (f) ΔDIC.

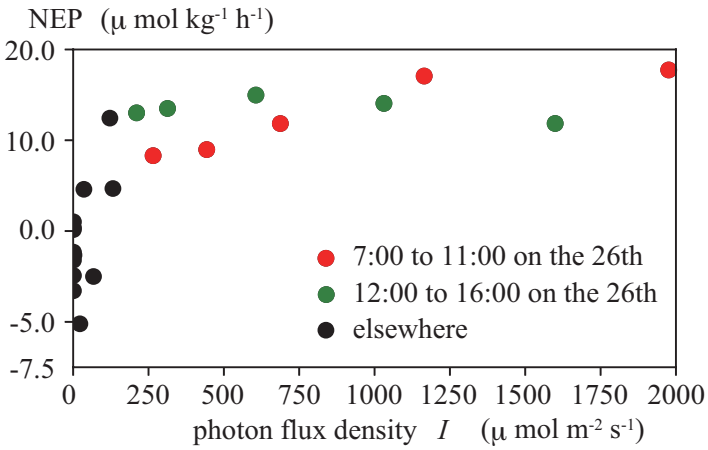

Fig. 4. Photon flux density and NEP.

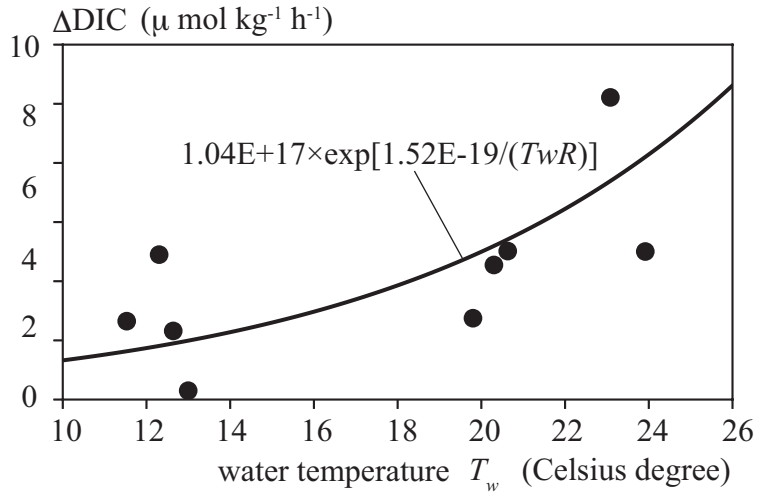

Fig. 5. Water temperature and ΔDIC. Solid line is the first term of equation (1).

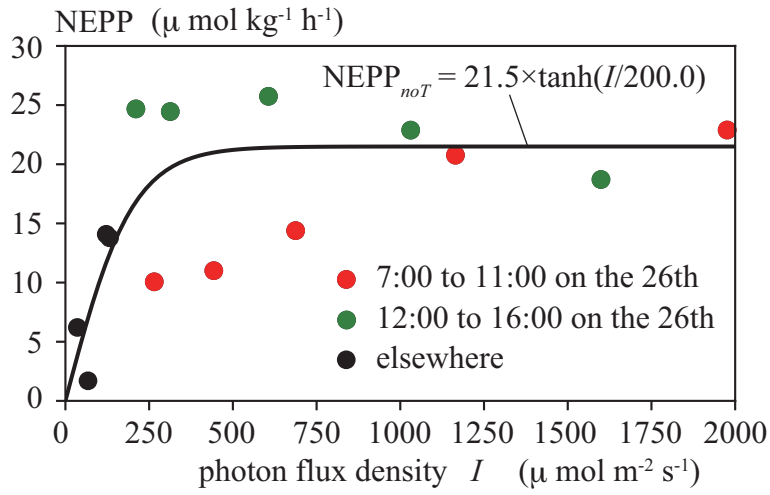

665

666 Fig. 6. Photon flux density and NEPP by equation (2). Solid line is equation (3).

667

668

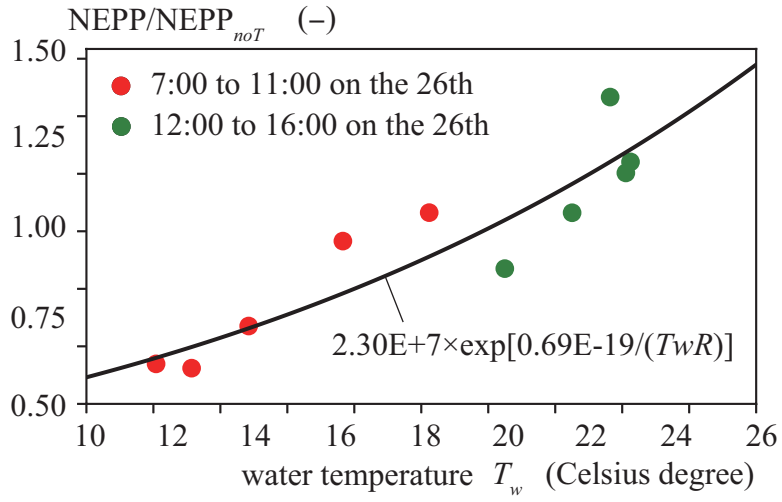

669

670 Fig. 7. Water temperature and the ratio of NEPP and NEPP$_{noT}$. Solid line is equation (4).

671

672

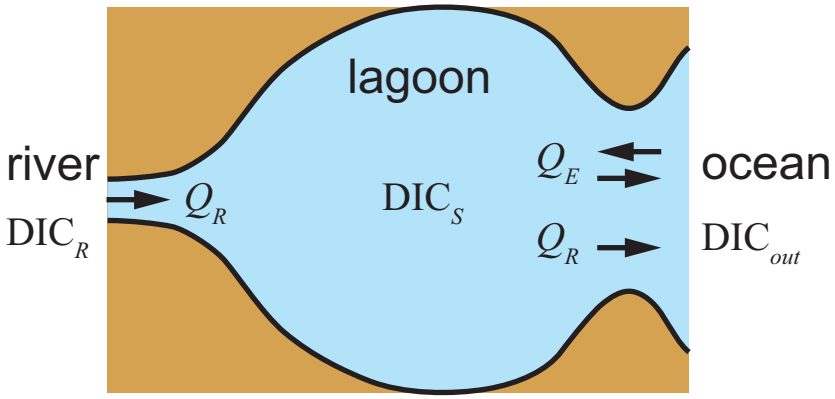

673

674 Fig. 8. Schematic diagram of SNEP model.

675

676

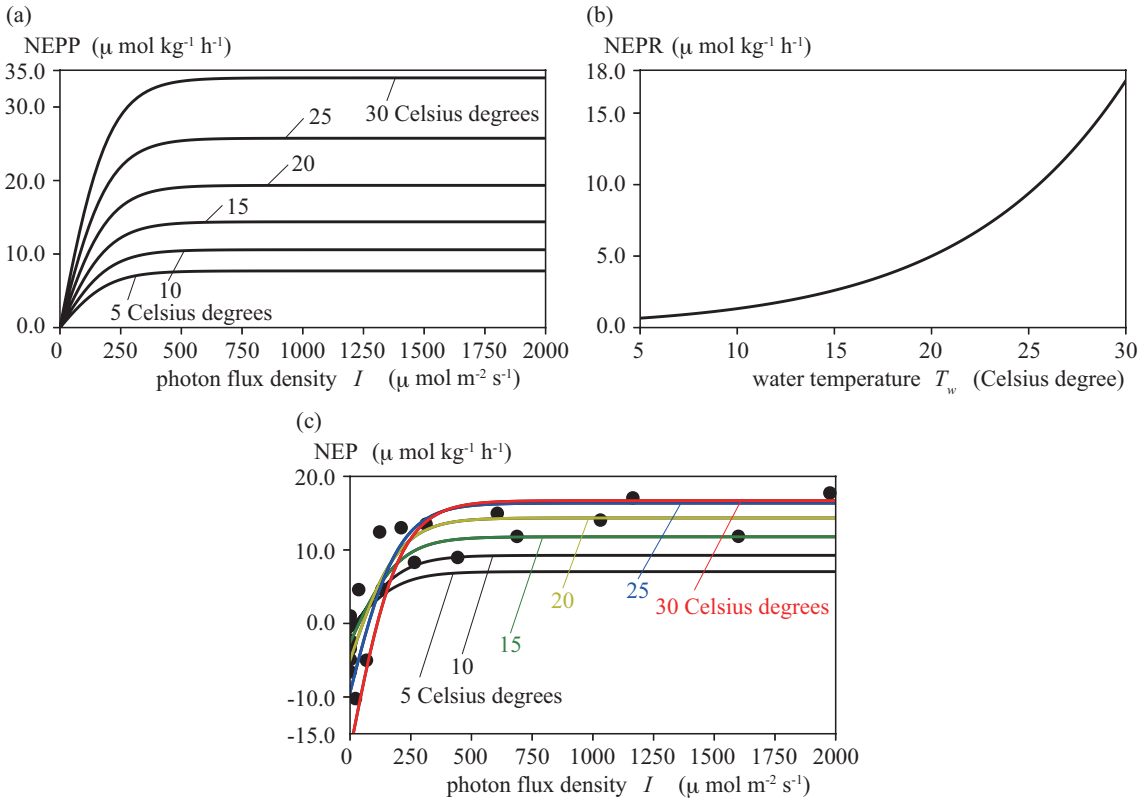

677

678 Fig. 9. Effect of water temperature on (a) NEPP, (b) NEPR and (c) NEP.

679

680

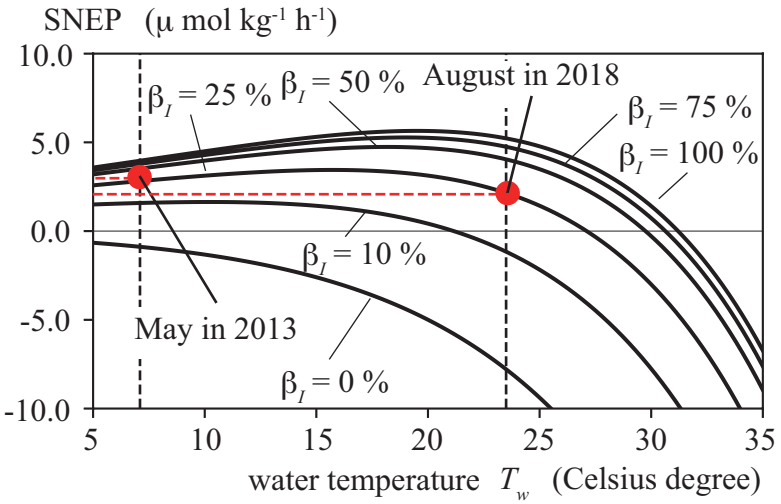

Fig. 10. Water temperature and DNEP in Komuke Lagoon.

685 Table 1. Specimens in laboratory experiments.

Eelgrass No.	Dry weight (leaf) (g)	Leaf biomass (g C/m^2)
1	379.94	253.15
2	419.07	284.27
3	490.96	325.87

686

687

688 Table 2. Nutrient concentrations in experimental water.

Water sample	NO_3-N (μM)	NO_2-N (μM)	NH_4-N (μM)	PO_4-P (μM)
Before experiment	1.642	0.100	2.127	0.804
After experiment	0.899	0.079	0.671	0.565

689

690

691 Table 3. γ_R and γ_P in May 2013 and August 2018.

β_I	100%	75%	50%	25%	10%	0%
γ_R	1.01					
γ_P (May in 2013)	0.56	0.54	0.51	0.42	0.28	0
γ_P (August in 2018)	0.54	0.52	0.49	0.42	0.28	0
γ_P (mean)	0.55	0.53	0.50	0.42	0.28	0

692

693

694 Table 4. Field observations in Lake Komuke.

	Mean water temperature (Celsius degree)	t_S (h)	ΔDIC_S (μ mol kg^{-1}) from observation	SNEP (μ mol kg^{-1} h^{-1}) from (7)	t_S SNEP (μ mol kg^{-1})
May 2013	7.1	110	325	2.82	310
August 2018	23.5	110	255	2.23	245

695

696

697

698